Progress In Electromagnetics Research M, Vol. 65, 187–195, 2018

An Electronically Tunable Dual-Band Filtering Power Divider with Tuning Diodes Sharing Technique

Yuan Jiang, Xian Qi Lin*, Cong Tang, and Jia Wei Yu

Abstract—This paper presents an electronically tunable dual-band filtering power divider (TDFPD) with tuning diodes sharing technique. Two dual-mode tunable resonators (DMTRs) are embedded into a conventional power divider to achieve dual-band tunable bandpass filtering response. The two bands of the proposed TDFPD can be tuned independently. Tuning diodes sharing technique is utilized to reduce the number of tunable diodes. A prototype has been designed and fabricated to validate the proposed design as shown by the good agreement between the measured and simulated results. The measurement shows that the center frequencies of the lower and upper bands can be independently tuned from 1.31 to 1.62 GHz and 2.92 to 3.30 GHz, respectively. Within the passbands, isolation between the two output ports is higher than 16 dB with small phase and magnitude imbalance.

1. INTRODUCTION

Multi-functionality is a trend in the development of RF/microwave components in modern wireless communication systems. However, multi-functional components may suffer from a large size and big design complexity. Tunable components, such as tunable filters [1–4], and function-merged components, such as filtering power dividers [5, 6], are effective to moderate the problems mentioned above. Tunable filters can achieve tunable passbands [1, 2], stopbands [3] or multi-functional performance [4], and filtering power dividers can be realized by embedding resonators into the power division arms [5, 6].

Tunable filtering power dividers, integrating the two types of components, have attracted much attention in [7–15]. [7–10] present that filtering power dividers are tuned by varactors, each of them having one tunable passband. Tunable filtering power dividers with constant absolutely bandwidth are reported in [7], and controllable bandwidth is reported in [8]. However, the number of varactors to ports ratio, in [7–10], is no less than 1, which involves a more complex bias circuit and higher cost. A tunable filtering power divider, utilizing a piezoelectric linear actuator, is reported in [11], whereas the size of the actuator is very bulky. Filtering power dividers with multiple passbands are achieved in [12–15]. As presented in [12], the switching between two passbands is realized by PIN diodes, and the bands cannot be tuned continuously. Power dividers with dual-band/multi-band tunable filtering performances are achieved in [13–15]. Tunable filtering power dividers, reported in [14, 15], integrate multi-functions of frequencies and bandwidths controlling for both pass and stopbands. However, none of them employed electronically tuning technique which is most commonly used in modern wireless systems, for example using varactors. The multiple tuning bands filtering power dividers are implemented by replacing fixed capacitors [13, 14] or using mechanically-adjustable capacitors [15]. That requires a technical intervention on trimmers. To the best of the authors' knowledge, there is no filtering power divider with multiple tuning bands implemented by electronically tuning technique reported previously.

Received 9 January 2018, Accepted 8 March 2018, Scheduled 20 March 2018

* Corresponding author: Xian Qi Lin (xqlin@uestc.edu.cn).

The authors are with the EHF Key Laboratory of Fundamental Science, School of Electronic Engineering, University of Electronic Science and Technique of China, Chengdu 611731, People's Republic of China.

In this paper, a multi-functional power divider with a filtering property and electronically tunable working frequencies is proposed. The number of tuning diodes is reduced by the tuning diodes sharing technique. A DMTR with two independently controllable modes is utilized to realize filtering function. Theoretical analysis of the DMTR is deduced to illustrate the tuning mechanism. For verification, a prototype with only three varactors is designed and fabricated. The two passbands can be tuned from 1.31 to 1.62 GHz and 2.92 to 3.30 GHz independently.

2. ANALYSIS OF THE TDFPD

Figure 1 shows the schematic of the proposed TDFPD. It consists of a "T" type input coupling circuit, a "Π" type output coupling circuit, a varactor diode (C_1) and two varactor-loaded microstrip lines (VML). The "T" type input coupling circuit and "Π" type output coupling circuit are connected by C_1 and two VMLs at the center, upside and downside, respectively. The input and output ports have the same reference characteristic impedance of the input and output lines Z_0. The coupled line of the input coupling circuit (CL-I) is identical to that of output coupling circuit (CL-O). The isolation resistor (R) connects port2 and port3. Varactors C_2 are placed at the center of the VMLs whose characteristic impedance is Z_m, and the electrical length is θ_m. The even-odd mode analysis technique [16] has been employed to develop and study the proposed circuitry. For each coupled line, the odd-mode impedance, even-mode impedance, and electrical length are denoted by Z_{0o}, Z_{0e} and θ, respectively.

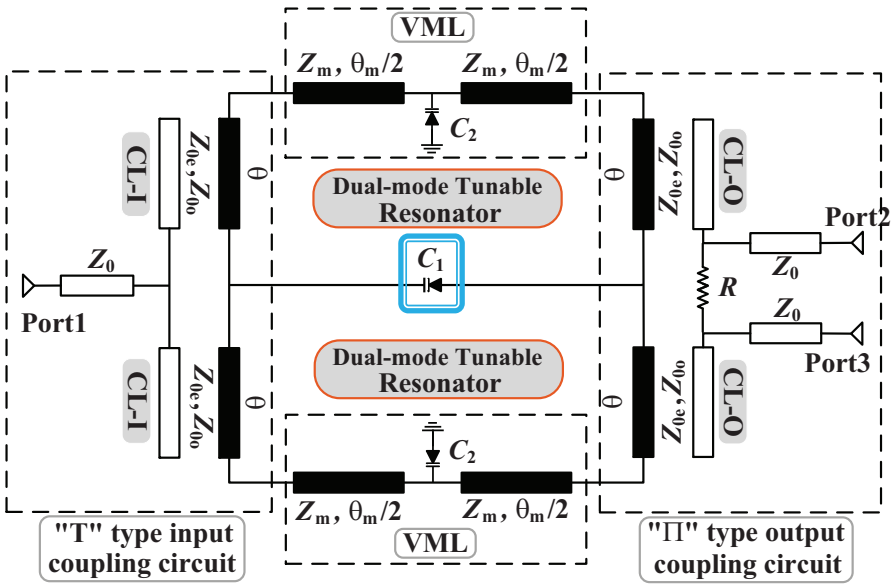

Figure 1. Schematic of the proposed TDFPD.

2.1. Tuning Diodes Sharing Technique

There are two power division arms, consisting of CL-I, CL-O, VML and shared C_1, in the proposed TDFPD. To explain the sharing technique, a basic TDFPD schematic is given in Figure 2(a). Two power division arms of the basic TDFPD are separated, by means of the Miller's theorem [17]. C_1 is replaced by two varactors $C_1/2$, compared with the proposed TDFPD shown in Figure 1. The circuit can be decomposed into a superposition of even-mode and odd-mode circuits, according to the even-odd mode analysis technique [16]. It can be seen that the proposed TDFPD and basic TDFPD have the same even- and odd-mode circuits from Figure 2(b). Therefore, the varactor diode C_1 can be shared by the two resonators retaining the same circuit response.

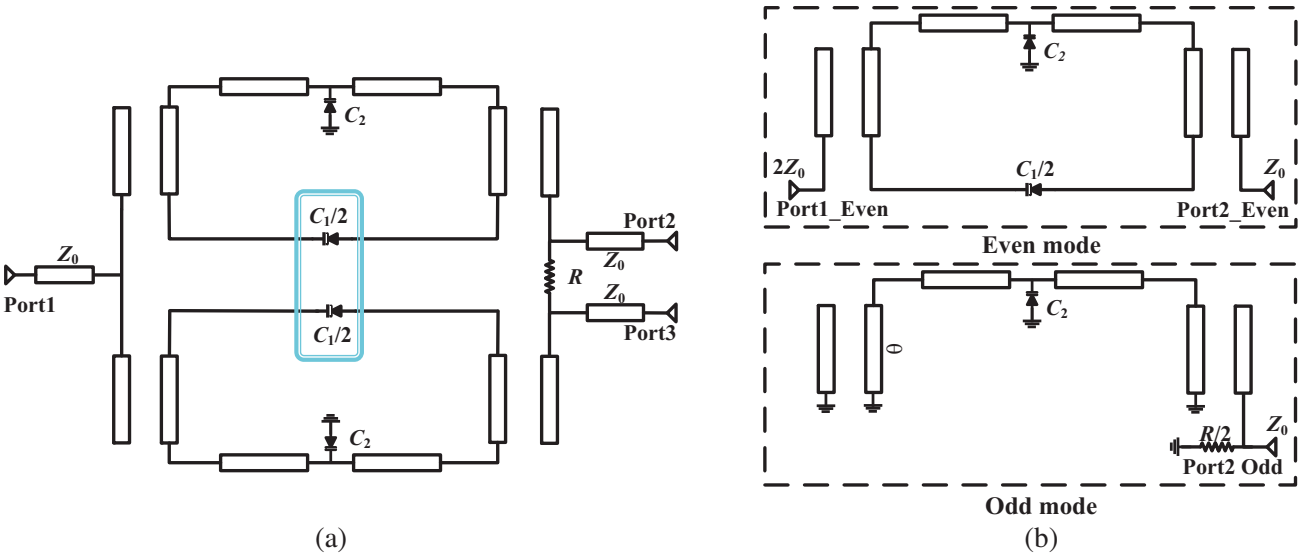

Figure 2. Schematic of (a) the basic TDFPD, (b) even- and odd-mode circuits of the proposed and the basic TDFPD.

2.2. Mechanism of Independent DMTR

The tunable filtering response of the TDFPD is achieved by embedding two identical DMTRs into each power division arm of a two-way power divider. This DMTR consists of halves of CL-I and CL-O, C1 and two VMLs (shown in Figure 1 filled with black). Figure 3(a) shows the schematic of the DMTR alone.

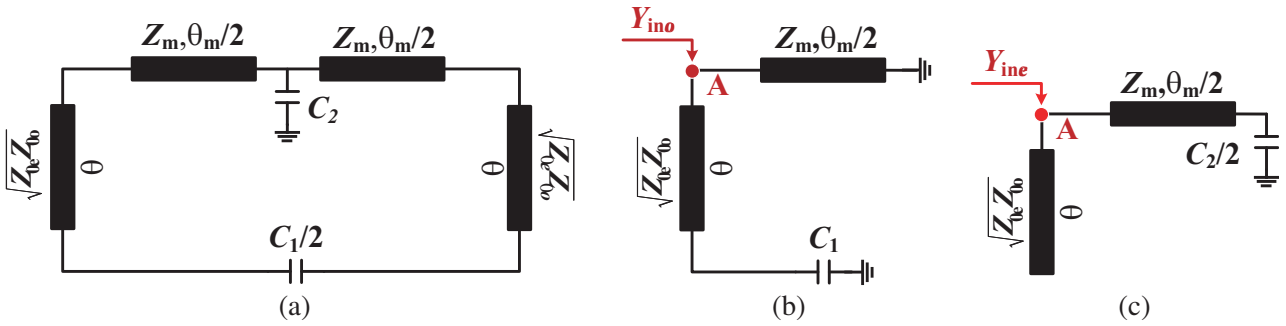

Figure 3. Schematic of the DMTR: (a) DMTR, (b) even-mode and (c) odd-mode.

Even-odd mode analysis is applied to analyze the resonant frequency of the DMTR. The even- and odd-mode circuits are shown in Figure 3(b) and Figure 3(c), respectively. The even- and odd-mode input admittance of point A can be derived as:

$$Y_{ine}(f) = j\left[\frac{\tan\left(\theta\frac{f}{f_0}\right)}{\sqrt{Z_{0e}Z_{0o}}} + \frac{2\pi f C_2 Z_m + 2\tan\left(\frac{\theta_m}{2}\frac{f}{f_0}\right)}{2Z_m - 2\pi f C_2 Z_m^2 \tan\left(\frac{\theta_m}{2}\frac{f}{f_0}\right)}\right], \tag{1}$$

$$Y_{ino}(f) = j\left[\frac{2\pi f\sqrt{Z_{0e}Z_{0o}}C_1 + \tan\left(\theta\frac{f}{f_0}\right)}{\sqrt{Z_{0e}Z_{0o}} - 2\pi f Z_{0e}Z_{0o}C_1\tan\left(\theta\frac{f}{f_0}\right)} - \frac{\cot\left(\frac{\theta_m}{2}\frac{f}{f_0}\right)}{Z_m}\right]. \tag{2}$$

When they meet the resonant condition:

$$Y_{\text{ine}}\left(f_{even}\right) = 0, \tag{3}$$

$$Y_{\text{ine}}\left(f_{even}\right) = 0, \tag{4}$$

the even- and odd-mode resonant frequency (f_{even} and f_{odd}) can be obtained as:

$$\frac{\tan\left(\theta\dfrac{f_{even}}{f_0}\right)}{\sqrt{Z_{0e}Z_{0o}}} + \frac{2\pi f_{even}C_2Z_{\text{m}} + 2\tan\left(\dfrac{\theta_{\text{m}}}{2}\dfrac{f_{even}}{f_0}\right)}{2Z_{\text{m}} - 2\pi f_{even}C_2Z_{\text{m}}^2\tan\left(\dfrac{\theta_{\text{m}}}{2}\dfrac{f_{even}}{f_0}\right)} = 0, \tag{5}$$

$$\frac{2\pi f_{odd}\sqrt{Z_{0e}Z_{0o}}C_1 + \tan\left(\theta\dfrac{f_{odd}}{f_0}\right)}{\sqrt{Z_{0e}Z_{0o}} - 2\pi f_{odd}Z_{0e}Z_{0o}C_1\tan\left(\theta\dfrac{f_{odd}}{f_0}\right)} - \frac{\cot\left(\dfrac{\theta_{\text{m}}}{2}\dfrac{f_{odd}}{f_0}\right)}{Z_{\text{m}}} = 0. \tag{6}$$

From Equations (5) and (6), it is observed that f_{even} only depends on C_2 while f_{odd} only depends on C_1. It means that the even and odd mode resonant frequencies can be tuned independently.

Full-wave simulation is carried out using Ansys's High Frequency Structural Simulator (HFSS) in order to verify the analysis above. The varactors are modeled as serial lumped RLC boundaries (resistors: $R_s = 0.8\,\Omega$, inductors: $L_s = 0.7\,\text{nH}$, and capacitors are according to the status of the varactors). An air box with a radiation boundary is used to simulate the open test environment. The DMTR is weakly coupled with two $50\,\Omega$ microstrip lines to investigate its resonant behaviour. Figure 4 shows the resonant frequencies of the dual-mode resonator. The even-mode resonant frequency is fixed at 3.31 GHz with $C_2 = 0.5\,\text{pF}$, and odd-mode resonant frequency is tuned from 1.46 to 1.13 GHz, when C_1 is varied from 0.5 to 1.5 pF as shown in Figure 4(a). On the other hand, the even-mode resonant frequency is changed from 2.78 to 3.31 GHz varying C_2 from 1.5 to 0.5 pF, and the odd-mode resonant frequency is fixed at 1.46 GHz with $C_1 = 0.5\,\text{pF}$, shown in Figure 4(b). Hence, the two passbands can be controlled independently since they are exclusively related to f_{odd} and f_{even}.

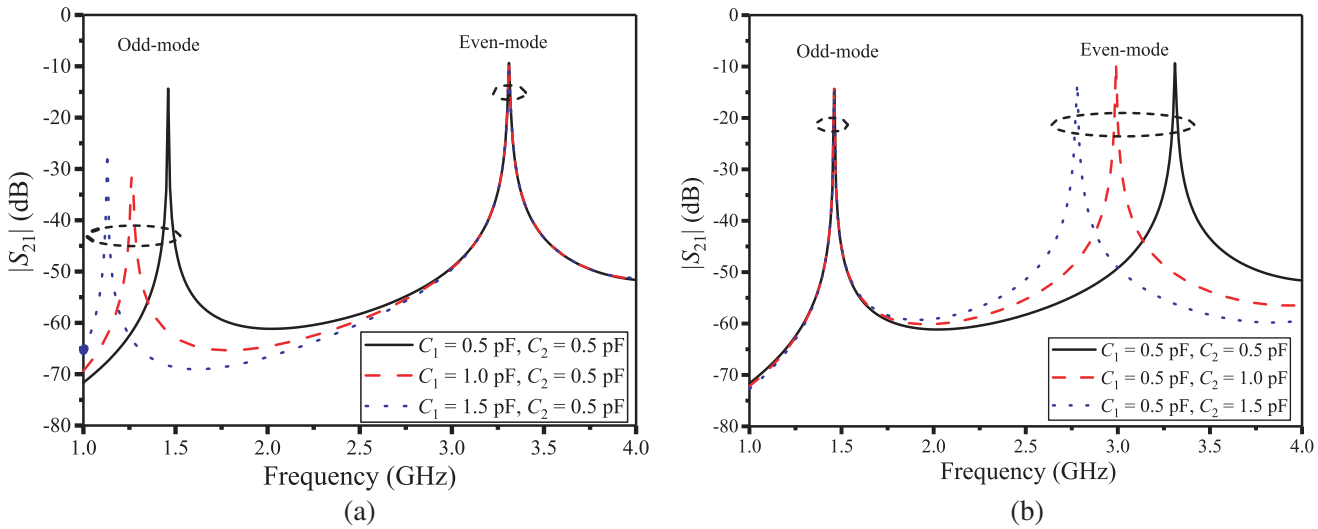

Figure 4. Resonant frequencies of the DMTR: (a) $|S_{21}|$ ($C_2 = 0.5\,\text{pF}$, $C_1 = 0.5$, 1.0 and 1.5 pF), (b) $|S_{21}|$ ($C_1 = 0.5\,\text{pF}$, $C_2 = 0.5$, 1.0 and 1.5 pF).

2.3. Study of the Proposed TDFPD

To study the performance of the TDFPD, the parameters of the proposed RFRPD are initialized as follows: $Z_0 = 50\,\Omega$, $Z_{0o} = 40\,\Omega$, $Z_{0e} = 130\,\Omega$, $Z_m = 40\,\Omega$, $\theta = 90°$, $\theta_m = 70°$, $R = 100\,\Omega$. Independently

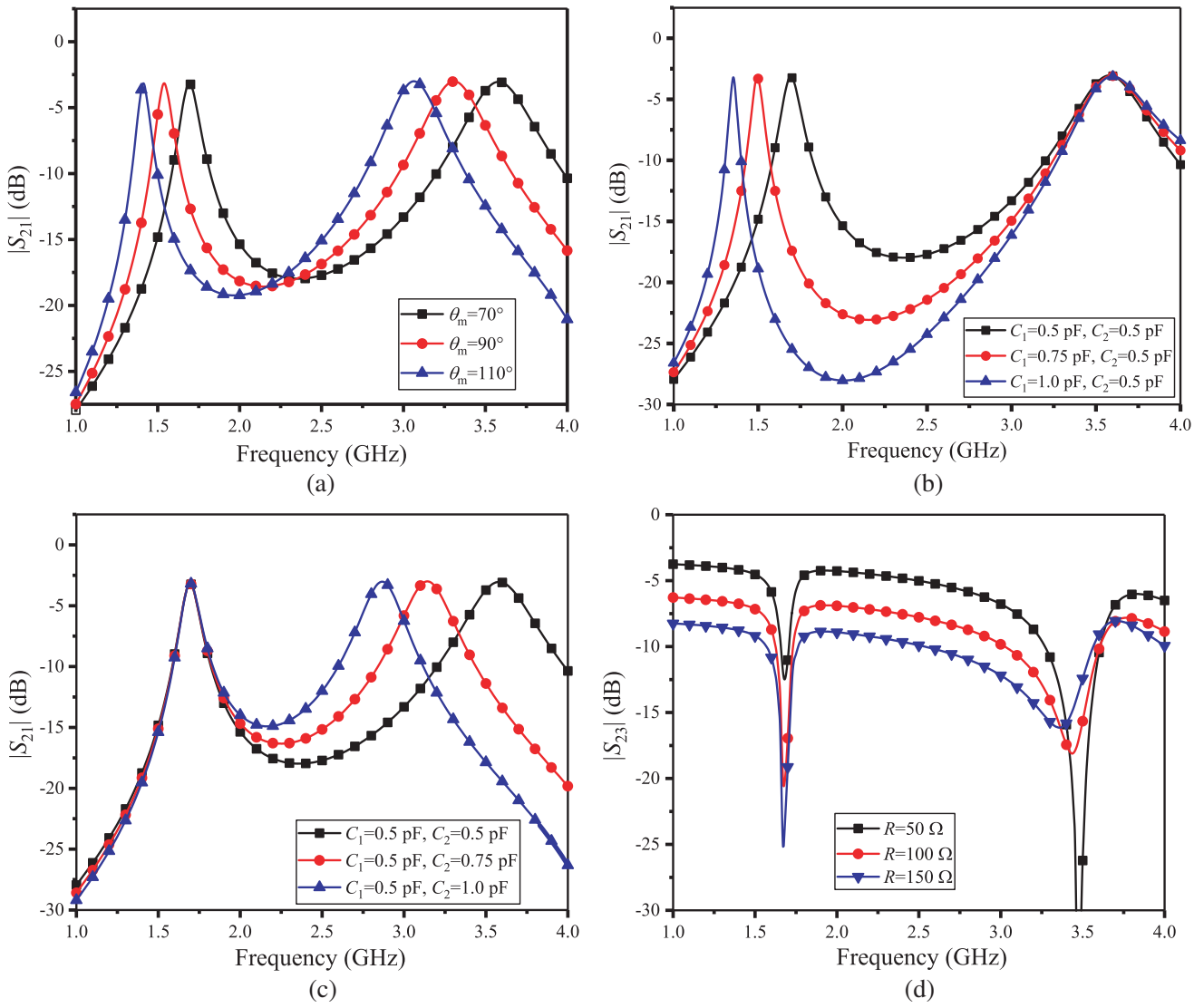

Figure 5. The performance study of the proposed TDFPD: (a) $|S_{21}|$ ($C_2 = 0.5$ pF, $C_1 = 0.5$, 0.75 and 1.0 pF), (b) $|S_{21}|$ ($C_1 = 0.5$ pF, $C_2 = 0.5$, 0.75 and 1.0 pF), (c) $|S_{21}|$ ($\theta_m = 70°$, 90° and 110°), (d) $|S_{23}|$ ($R = 50$, 100 and 150 Ω).

controllable passbands versus C_1 and C_2 are shown in Figures 5(a) and (b). As shown in Figure 5(a), the lower band is shifted down as C_1 increases with the upper band fixed with $C_2 = 0.5$ pF. The lower band is fixed with $C_1 = 0.5$ pF, while the upper band is changed by varying C_2, shown in Figure 5(b). Figure 5(c) compares the resonant frequencies under different θ_m, when C_1 and C_2 are fixed at 0.5 pF. It is observed that both the lower and upper bands are shifting toward lower frequency bands when θ_m is becoming larger. This property makes θ_m a good parameter to set the tuning range of the TDFPD. Figure 5(d) shows the isolation between port2 and port3 against the resistor R. A larger R improves the isolation of the lower band but also worsens that of the upper band. Therefore, a median of $R = 100\,\Omega$ is selected to compromise the isolations of both lower and upper bands.

3. MEASUREMENT OF THE PROPOSED TDFPD

A TDFPD prototype is designed and fabricated to verify the proposed idea. The corresponding dimensions are shown in Figure 6(a). Figure 6(b) presents the fabricated prototype with the overall size

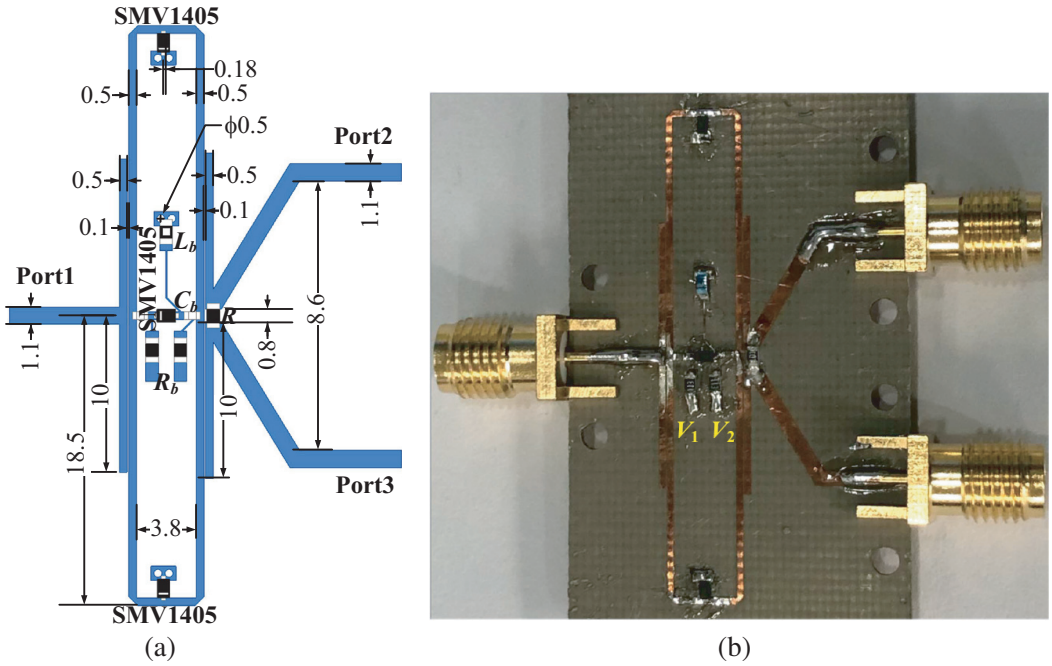

Figure 6. (a) Dimensions (unit: mm) and (b) photograph of the TDFPD prototype.

of $43.0 \times 26.4\,\text{mm}^2$. The circuit is designed on a Taconic RF-35 substrate with a thickness of 0.508 mm, relative permittivity of $\varepsilon_r = 3.5$ and dielectric loss tangent of $\delta = 0.0018$. Skyworks SMV1405 is utilized as tuning diodes. The bias resistor $R_b = 11\,\text{k}\Omega$, inductor $L_b = 20\,\text{nH}$, capacitor $C_b = 5\,\text{pF}$, and the isolation resistor (R) is $100\,\Omega$. V_1 and V_2 represent the voltage applied to varactors C_1 and C_2, respectively. HFSS is used to simulate and optimize the design performance.

The measured results are in good agreement with the simulated ones, shown in Figure 7. As can be seen, the lower band of the TDFPD can be tuned from 1.31 to 1.62 GHz when the voltage of C_1 is varied from 8 V to 30 V, and C_2 is biased at 30 V as shown in Figures 7(a), (c) and (e). Within the tuning range of the lower band, the measured $|S_{21}|$ and $|S_{31}|$ are both lower than 7.8 dB and reach a minimum of 5.5 dB at 1.62 GHz indicating that the loss caused by the filtering and power division is 2.5 to 4.8 dB. Figures 7(b), (d) and (f) show that the upper band of the TDFPD can be tuned from 2.92 to 3.30 GHz when the voltage of C_2 is varied from 13 V to 30 V, and C_1 is biased at 30 V.

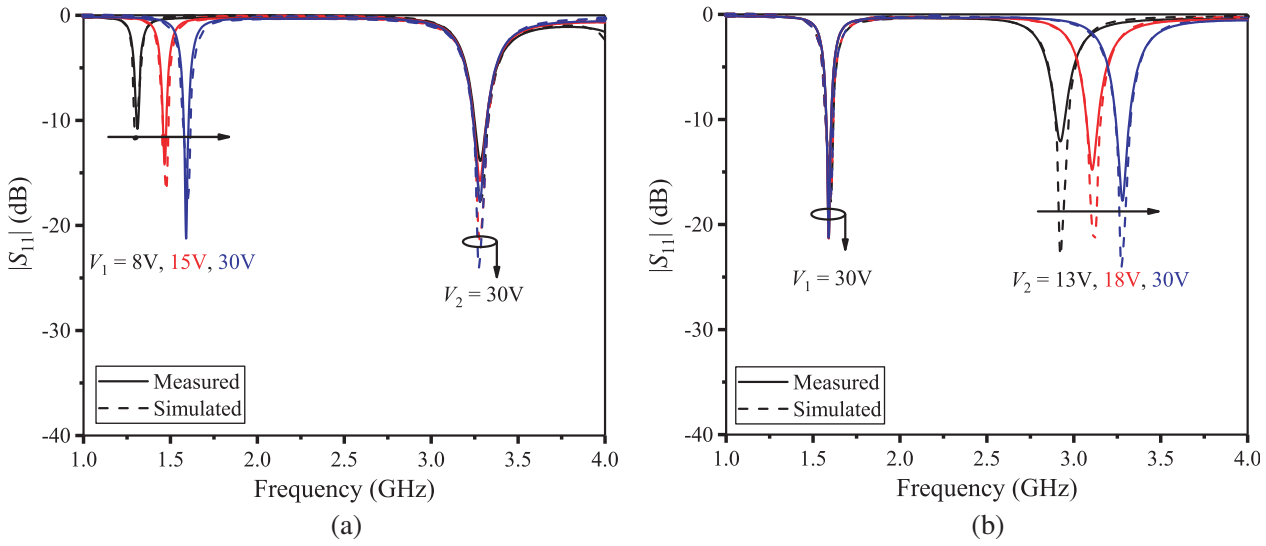

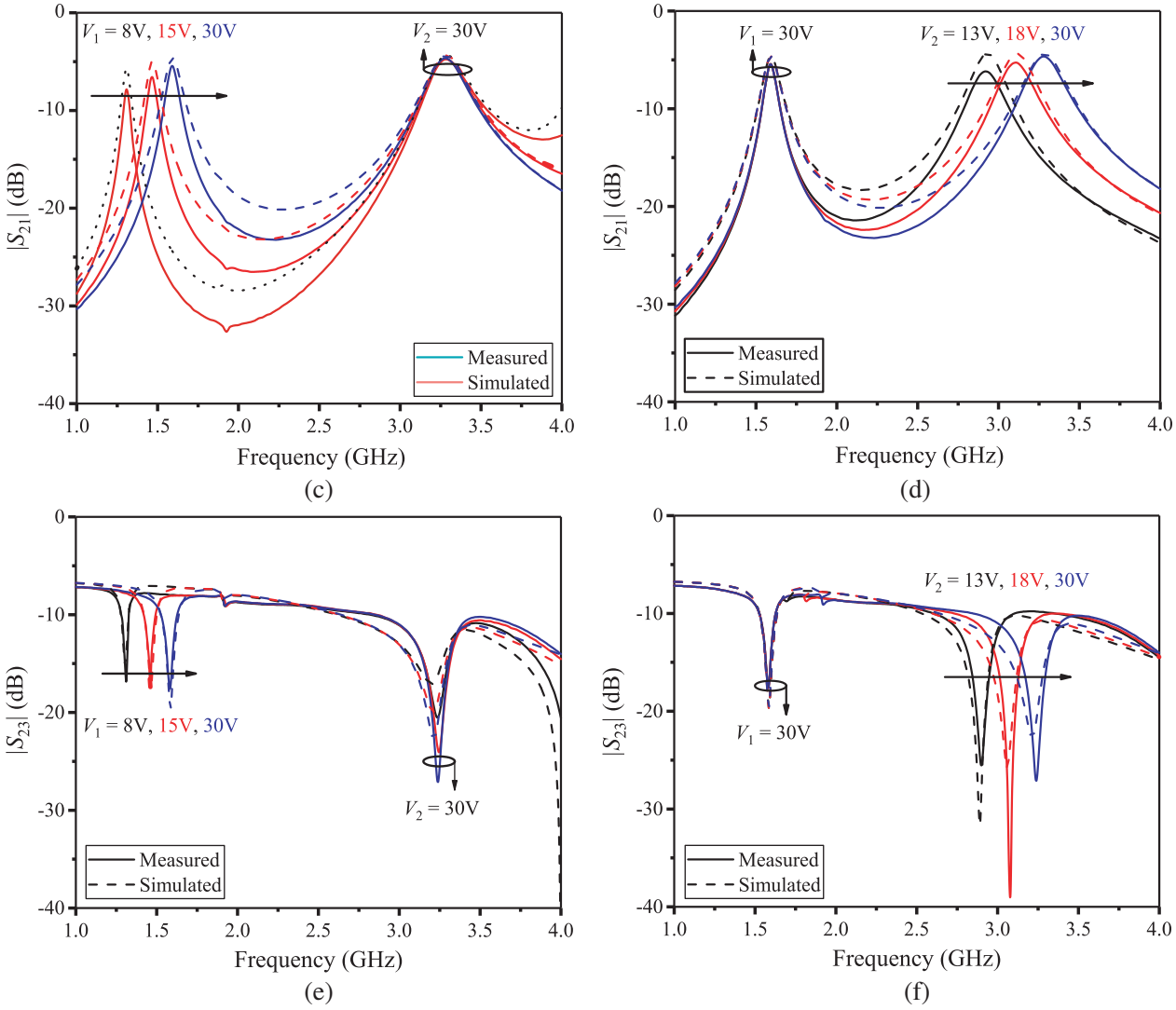

Figure 7. Simulated and measured results: (a), (b) and (c): $V_2 = 30\,\text{V}$, $V_1 = 8\,\text{V}$, $15\,\text{V}$ and $30\,\text{V}$, (d), (e) and (f): $V_1 = 30\,\text{V}$, $V_2 = 13\,\text{V}$, $18\,\text{V}$ and $30\,\text{V}$.

Within the tuning range of the upper band, the loss caused by the filtering and power division is 1.7 to 3.2 dB. The return loss is better than 12 dB, and isolation between port 2 and port 3 is larger than 16 dB over the tuned passbands. Within the passbands, the magnitude imbalance and phase difference are, respectively, about ± 0.5 dB and ± 2.0 deg as shown in Figure 8. The small differences are mainly contributed by the inconsistencies of the varactors and fixtures connected to the two output ports.

As can be deduced from Equations (5) and (6) and discussed in the previous section, the number of tuning diodes will increase with the number of bands and output ports. It is a critical issue to reduce the number of tuning diodes because increasing tuning elements will raise the cost, complexity and some other bad influence of the circuit. So, we define a factor:

$$TPBR = \frac{Number\ of\ tunning\ diodes}{Number\ of\ output\ ports \times Number\ of\ tunable\ bands}, \tag{7}$$

to evaluate the usage of tunning diodes due to the increasing number of output ports and bands:

The proposed two-way dual-band filtering power divider has three varactors which means that $TPBR = 3/(2 * 2)$ is only 0.75. Compared with some other tunable filtering power dividers in Table 1, assuming that the power dividers of [13, 15] are electronically tuned by varactors, the proposed TDFPD has the lowest $TPBR$, less than 1.

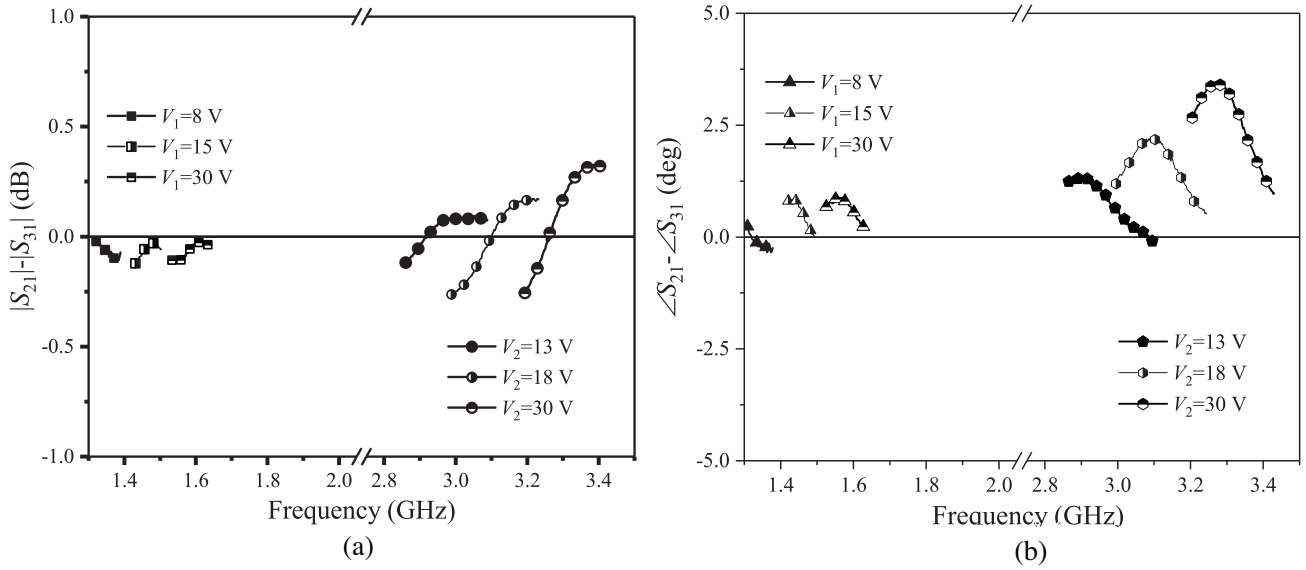

Figure 8. Measured results of (a) magnitude imbalance and (b) phase difference.

Table 1. Comparison with some other tunable filtering power dividers.

	Freq (GHz)	IL (dB)	ISO. (dB)	Tunable methods	No. of bands	No. of ports	No. of diodes	TPBR
[7]	0.62–0.85	1.8–2.4	> 16	Electronically	1	2	6	3.0
[8]	1.30–2.08	2.9–5.3	> 26	Electronically	1	2	12	6.0
[13]	0.66–0.99	0.8–2.3	> 12	Manually replacing fixed capacitors	2	2	4	$1.0^{(a)}$
	1.6–1.94	1.2–1.8						
[15]	0.85–1.01	< 2	> 30	Using mechanically-adjustable capacitors	2	2	6	$1.5^{(b)}$
	0.96–1.16	< 2						
This work	1.31–1.62	2.5–4.8	> 16	Electronically	2	2	3	**0.75**
	2.92–3.30	1.7–3.2						

(a) Assuming that the fixed capacitors were replaced by varactors.
(b) Assuming that the mechanically-adjustable capacitors were replaced by varactors and that the filtering power divider is working under dual-band tunable mode.

4. CONCLUSION

An electronically tunable dual-band filtering power divider is introduced in this paper. The lower passband can be tuned from 1.31 to 1.62 GHz while the tuning range of the upper passband is from 2.92 to 3.30 GHz by using two DMTRs. In addition, the two bands can be controlled independently. Furthermore, the quantity of the varactors can be reduced by utilising tuning diodes sharing technique. Compared with all the previous researches on tunable filtering power dividers, the proposed filtering power divider has an ultra-small *TPBR* of 0.75. The simulation and measurement agree well benefited from the even-odd mode analysis. The proposed filtering power divider and tuning diodes sharing technique can be applied in tunable microwave systems.

ACKNOWLEDGMENT

This work was supported in part by NSFC (No. 61571084), in part by EPRF (No. 6141B06120101), in part by NDSTI (No. 1716313ZT00802902), and in part by NKIF (No. 2017510007000006).

REFERENCES

1. Schuster, C., A. Wiens, F. Schmidt, M. Nickel, M. Schubler, R. Jakoby, and H. Maune, "Performance analysis of reconfigurable bandpass filters with continuously tunable center frequency and bandwidth," *IEEE Trans. Microw. Theory Tech.*, Vol. 65, No. 11, 4572–4583, Nov. 2017.
2. Leggieri, A., D. Passi, D. Gagliesi, and F. D. Paolo, "Analysis and design of a gaas monolithic tunable polyphase filter in s/c bands," *J. Microw. Optoelectron. Electromagn. Appl.*, Vol. 14, No. 1, 14–27, Jun. 2015.
3. Gómez-García, R., D. Psychogiou, and D. Peroulis, "Fully-tunable filtering power dividers exploiting dynamic transmission-zero allocation," *IET Microw. Antennas Propag.*, Vol. 11, No. 3, 378–385, Feb. 2017.
4. Feng, W., Y. Shang, W. Che, R. Gomez-Garcia, and Q. Xue, "Multifunctional reconfigurable filter using transversal signal-interaction concepts," *IEEE Microw. Wireless Compon. Lett.*, Vol. 27, No. 11, 980–982, Nov. 2017.
5. Zhao, X., K. Song, Y. Zhu, and Y. Fan, "Wideband four-way filtering power divider with isolation performance using three parallel-coupled lines," *IEEE Microw. Wireless Compon. Lett.*, Vol. 27, No. 9, 800–802, Sep. 2017.
6. Chen, F. J., L. S. Wu, L. F. Qiu, and J. F. Mao, "A four-way microstrip filtering power divider with frequency-dependent couplings," *IEEE Trans. Microw. Theory Tech.*, Vol. 63, No. 10, 3494–3504, Oct. 2015.
7. Gao, L., X. Y. Zhang, and Q. Xue, "Compact tunable filtering power divider with constant absolute bandwidth," *IEEE Trans. Microw. Theory Tech.*, Vol. 63, No. 10, 3505–3513, Oct. 2015.
8. Chi, P. L. and T. Yang, "A 1.3–2.08 GHz filtering power divider with bandwidth control and high in-band isolation," *IEEE Microw. Wireless Compon. Lett.*, Vol. 26, No. 6, 407–409, Jun. 2016.
9. Lin, S.-C., Y.-M. Chen, P.-Y. Chiou, and S.-F. Chang, "Tunable Wilkinson power divider utilizing parallel-coupled-line-based phase shifters," *IEEE Microw. Wireless Compon. Lett.*, Vol. 27, No. 4, 335–337, Apr. 2017.
10. Lee, B., B. Koh, S. Nam, T. H. Lee, and J. Lee, "Frequency-tunable filtering power divider with new topology," *IEEE Trans. Compon. Packag. Manuf. Technol.*, Vol. 7, No. 7, 1151–1162, Jul. 2017.
11. Wong, K. W., R. R. Mansour, and G. Weale, "Reconfigurable bandstop and bandpass filters with wideband balun using IPD technology for frequency agile applications," *IEEE Trans. Compon. Packag. Manuf. Technol.*, Vol. 7, No. 4, 610–620, Apr. 2017.
12. Zhu, C., J. Xu, W. Kang, and W. Wu, "Microstrip switchable filtering power divider with three operating modes," *Electron. Lett.*, Vol. 52, No. 25, 2046–2048, Dec. 2016.
13. Lu, Y., G. Dai, Y. Wang, T. Liu, and J. Huang, "Dual-band filtering power divider with capacitor-loaded centrally coupled-line resonators," *IET Microw. Antennas Propag.*, Vol. 11, No. 1, 36–41, Jan. 2017.
14. Psychogiou, D., R. Gómez-García, and D. Peroulis, "Fully adaptive multiband bandstop filtering sections and their application to multifunctional components," *IEEE Trans. Microw. Theory Tech.*, Vol. 64, No. 12, 4405–4418, Dec. 2016.
15. Psychogiou, D., R. Gómez-García, A. C. Guyette, and D. Peroulis, "Reconfigurable single/multiband filtering power divider based on quasi-bandpass sections," *IEEE Microw. Wireless Compon. Lett.*, Vol. 26, No. 9, 684–686, Dec. 2016.
16. Pozar, D. M., *Microwave Engineering*, 4th Edition, John Wiley & Sons, New York, NY, USA, 2009.
17. Moura, L. and I. Darwazeh, *Introduction to Linear Circuit Analysis and Modelling: From DC to RF*, 1st Edition, Elsevier, London, UK, 2005.